The Journal of Immunology

NF-κB-Driven STAT2 and CCL2 Expression in Astrocytes in Response to Brain Injury

Reza Khorooshi, Alicia A. Babcock and Trevor Owens

J Immunol 2008; 181:7284-7291; ;
doi: 10.4049/jimmunol.181.10.7284
http://www.jimmunol.org/content/181/10/7284

The Journal of Immunology is published twice each month by
The American Association of Immunologists, Inc.,
1451 Rockville Pike, Suite 650, Rockville, MD 20852

Print ISSN: 0022-1767 Online ISSN: 1550-6606.

NF-κB-Driven STAT2 and CCL2 Expression in Astrocytes in Response to Brain Injury[1]

Reza Khorooshi, Alicia A. Babcock, and Trevor Owens[2]

Tissue response to injury includes expression of genes encoding cytokines and chemokines. These regulate entry of immune cells to the injured tissue. The synthesis of many cytokines and chemokines involves NF-κB and signal transducers and activators of transcription (STAT). Injury to the CNS induces glial response. Astrocytes are the major glial population in the CNS. We examined expression of STATs and the chemokine CCL2 and their relationship to astroglial NF-κB signaling in the CNS following axonal transection. Double labeling with Mac-1/CD11b and glial fibrillary acidic protein revealed that STAT2 up-regulation and phosphorylation colocalized exclusively to astrocytes, suggesting the involvement of STAT2 activating signals selectively in astroglial response to injury. STAT1 was also up-regulated and phosphorylated but not exclusively in astrocytes. Both STAT2 up-regulation and phosphorylation were NF-κB -dependent since they did not occur in the lesion-reactive hippocampus of transgenic mice with specific inhibition of NF-κB activation in astrocytes. We further showed that lack of NF-κB signaling significantly reduced injury-induced CCL2 expression as well as leukocyte infiltration. Our results suggest that NF-κB signaling in astrocytes controls expression of both STAT2 and CCL2, and thus regulates infiltration of leukocytes into lesion-reactive hippocampus after axonal injury. Taken together, these findings indicate a central role for astrocytes in directing immune-glial interaction in the CNS injury response. ***The Journal of Immunology,*** **2008, 181: 7284–7291.**

The inflammatory response to tissue injury is critical for host protection and repair. Injury to the CNS induces activation of glial cells whose response is essential for maintenance of the neuronal environment and functions (1, 2). Astrocytes are the most abundant glial cell population in the CNS. They play a key role in regulation of CNS homeostasis by regulating ion, neurotransmitter, and growth factor levels, providing a supportive structure for neurons, and by influencing the formation and function of the blood-brain barrier (1, 3, 4).

Astrocytes contribute to the regulation of inflammatory responses in the CNS by producing an array of cytokines and chemokines (1, 4–8). These synergize with adhesion and other processes in regulating tissue inflammation. The chemokine MCP-1/CCL2 is particularly implicated in the recruitment of monocytes/macrophages and lymphocytes into the CNS (8, 9). Specifically, CNS-derived CCL2, acting through its receptor CCR2, has been shown to drive leukocyte infiltration in response to axonal injury in the brain (10). Although many cells in the CNS, including glia, neurons, and endothelial cells, can produce CCL2 (11, 12), and both microglia and astrocytes were identified by us as sources of CCL2 in response to injury (10), the relative contribution of astrocytes to injury-induced CCL2 expression and leukocyte infiltration in response to injury is not clear.

Receptor signaling that activates transcription factors such as NF-κB and STAT regulate transcription of many inflammatory mediators, including cytokines and chemokines (13–16). NF-κB signaling is activated in response to CNS injury (17–19). STAT1 and STAT2 have been shown to direct transcription of regulatory factors that are important for antiviral defense in the CNS (20). The cellular localization and regulation of STAT1 and STAT2 in response to axonal injury have not been studied.

We have examined the role of NF-κB and STAT1 and STAT2 signaling in the CCL2 response in the hippocampus following transection of axons in the entorhinal cortex. This is a widely used model of neuronal-glial interaction and injury-induced inflammation in the brain. In this model, transection of axons projecting to the hippocampus leads to synaptic degeneration in the outer molecular layer of the dentate gyrus, which induces activation of microglia and astrocytes, up-regulation of inflammatory mediators, and infiltration of macrophages and T cells (10, 21–26). We show that STAT2 was up-regulated in the denervated hippocampus after axonal lesion, and that its expression was exclusively localized to astrocytes. This induction of STAT2 in astrocytes was completely dependent on NF-κB. Inhibition of NF-κB in astrocytes led to significant reduction of injury-induced CCL2 response and leukocyte infiltration. Collectively, these findings point to astrocytes and astroglial NF-κB signaling as important factors influencing the inflammatory response to axonal injury in the CNS.

Materials and Methods

Animals

The following adult female (18–20 g) mice were used: mice deficient in STAT1 (STAT1-KO, 129s6/SvEv background (27)) were purchased from Taconic Europe, STAT2 (STAT2 deficient, 129s6/SvEv background (28)) were kindly provided by Dr. Chris Schindler (Columbia University, New York, NY) and bred in our facility, and glial fibrillary acidic protein (GFAP)-IκBα-dn (C57BL/6 background (19)) were kindly provided by Dr. John R. Bethea (Department of Neurological Surgery, University of Miami School of Medicine, FL) and bred in our

Medical Biotechnology Center, University of Southern Denmark, Odense, Denmark

Received for publication January 8, 2008. Accepted for publication September 20, 2008.

The costs of publication of this article were defrayed in part by the payment of page charges. This article must therefore be hereby marked *advertisement* in accordance with 18 U.S.C. Section 1734 solely to indicate this fact.

[1] This study was supported by grants to T.O. from the Danish Agency for Science, Technology and Innovation and from Novo Nordisk Fonden. A.B. was supported by Lundbeckfonden.

[2] Address correspondence and reprint requests to Dr. Trevor Owens, Medical Biotechnology Center, University of Southern Denmark, Winsloewparken 25, 5000 Odense C, Denmark. E-mail address: towens@health.sdu.dk

Table I. *List of primary and secondary Abs*

Primary Abs
Rabbit anti-STAT1 (SC-346; Santa Cruz Biotechnology)
Rabbit anti-STAT2 (SC-950; Santa Cruz Biotechnology)
Rabbit anti-phospho-STAT2 (Tyr^{689}) (07-224; Upstate Biotechnology)
Rabbit anti-phospho-STAT1 (07-307; Upstate Biotechnology)
Goat anti-GFAP (SC-6171; Santa Cruz Biotechnology)
Rat anti-mouse Mac-1/CD11b (MCA711; Serotec)
Rabbit anti-GFAP (Z0334; Dako)
Secondary Abs
Biotinylated goat anti-rabbit (Amersham Biosciences)
HRP-conjugated goat anti-rabbit IgG (A9169; Sigma-Aldrich)
Alexa 568-labeled goat anti-rat (A11077; Invitrogen)
Alexa 488-labeled goat anti-rabbit (A11034; Invitrogen)
Alexa 568-labeled donkey anti-goat (A11057; Invitrogen)
Alexa 488-labeled donkey anti-rabbit (A21206; Invitrogen)
Control Ab
Rabbit IgG (PRABP01; Serotec)

facility. Wild-type mice (WT)[3] (C57BL/6 and 129s6/SvEv) were purchased from Taconic (Taconic Europe). The genotypes of mice were verified by PCR analysis of tail DNA. Mice were provided with food and water ad libitum and were housed under pathogen-free conditions with a constant light/dark cycle. These experiments were conducted according to the guidelines of the National Danish Animal Research Committee.

Entorhinal cortex lesioning

Under anesthesia mice were placed in a Kopf stereotactic apparatus (Kopf Instruments) and a burr hole was drilled in the skull 1.9 mm lateral to lambda and 0.3 mm caudal to the lambdoid suture. The nosebar was set at −3 mm. A wire knife (Kopf Instruments) was inserted at an angle of 15° rostrally and 10° laterally, and 3.4 mm ventral to the meninges, the knife was unfolded and the entorhinodentate perforant path projection was sectioned by retracting the knife 3.2 mm (24, 29).

Tissue preparation

Mice were deeply anesthetized and perfused transcardially with 5 ml cold PBS followed by 20 ml cold 4% paraformaldehyde (Sigma-Aldrich) in PBS. The brains were removed and postfixed in PBS containing 4% paraformaldehyde for 2 h on ice, then immersed in 30% sucrose in PBS overnight at 4°C, frozen with CO_2 snow, and stored at −20°C until sectioning.

Brains were cut into parallel series of free-floating sections and stored in de Olmos cryoprotectant solution containing polyvinylpyrrolidone (Sigma-Aldrich) and sucrose diluted in a mixture of ethylene glycol (Merck) and of Na phosphate buffer (24) until further processing. Unmanipulated and contralateral hippocampi were used as controls.

Antibodies

Primary and secondary Abs are listed in Table I.

Immunohistochemistry

Free-floating sections were incubated in 1% H_2O_2 and 1% methanol diluted in PBS for 15 min to block endogenous peroxidases, followed by rinsing in PBS. The sections were then rinsed in PBS containing 0.5% Triton X-100 (PBST) (Sigma-Aldrich). After preincubation with blocking solution containing PBST and 3% BSA, the sections were incubated overnight with primary Ab diluted in blocking solution at 4°C. The following day, the sections were rinsed in PBST and incubated with secondary biotinylated Abs for 1 h at room temperature followed by rinsing in PBST. The sections were finally incubated with streptavidin-HRP (P0397, Dako) for 1 h at room temperature, rinsed in PBS, and developed with 0.5 mg/ml of diaminobenzidine (Sigma-Aldrich) for 5–10 min. After a quick rinse in PBS, sections were mounted on gelatinized glass slides, dried, dehydrated through ethanol, cleared in xylene, and coverslipped with DePeX (VWR International).

For phospho-STAT2 immunostaining, the tissue was pretreated with 1% NaOH and 1% H_2O_2 for 20 min, 0.3% glycine for 10 min, and 0.03% SDS (USB/Affymetrix) for 10 min at room temperature as described for phospho-STAT3 immunostaining (30). Sections were blocked for 30 min with blocking solution at room temperature and then incubated with anti-phospho-STAT2 Ab overnight at 4°C. The following day, the sections were rinsed in PBST and incubated with secondary biotinylated Abs for 1 h at room temperature followed by rinsing in PBST. The sections were finally incubated with streptavidin-HRP for 1 h at room temperature, rinsed in PBS, and developed with diaminobenzidine.

For dual-labeling immunofluorescence, free-floating sections were incubated with a cocktail containing primary Abs, rabbit anti-STAT2 and rat anti-mouse Mac-1/CD11b, or rabbit anti-STAT2 and goat anti-GFAP (Table I) diluted in blocking solution overnight at 4°C. The next day, sections were washed and incubated with a cocktail containing the corresponding fluorescent secondary Abs: Alexa 568-labeled goat anti-rat and Alexa 488-labeled goat anti-rabbit, or Alexa 568-labeled donkey anti-goat and Alexa 488-labeled donkey anti-rabbit (Table I) diluted in blocking solution for 1 h at room temperature.

Images were acquired using an Olympus BX51 microscope and an Olympus DP71 digital camera. Images were combined using Adobe Photoshop CS version 8.0, using RGB channels to visualize double-labeled cells.

Control sections were treated without primary Ab or with isotype-matched primary Abs. Control sections displayed no staining comparable with that seen with primary Abs (see Fig. 1, *E* and *F*).

Western blot analysis

Hippocampi were isolated from PBS-perfused mice and lysed in lysis buffer (200 μl) containing 50 mM Tris-HCl (pH 8.0), 1 mM EDTA, 150 mM NaCl, 1% Igepal 630 (Sigma-Aldrich), protease inhibitor cocktail (Roche), 1 mM Na_3VO_4 (Sigma-Aldrich), 4.5 mM sodium-pyrophosphate (Sigma-Aldrich), 10 mM β-glycerophosphate, and 1 mM NaF. Forty micrograms of cell lysate was mixed with an equal volume of sample buffer containing 62.5 mM Tris-HCl (pH 6.8), 10% glycerol, 2% SDS, 5% β-mercaptoethanol, and 2–3 drops of saturated bromophenol solution, denatured by boiling, and separated by electrophoresis in an 8–10% polyacrylamide gel at 60 V for 26 min, 120 V for 26 min, and 190 V for 35 min. The separated proteins were transferred at 250 mA for 1 h 20 min to a nitrocellulose membrane (Bio-Rad Laboratories). The membranes were blocked for 1 h at room temperature in 5% nonfat dry milk in PBS containing 0.1% Tween 20. The membranes were then incubated with primary rabbit Abs at 4°C overnight. After washing in PBST, the membranes were incubated with goat anti-rabbit IgG HRP conjugate (Sigma-Aldrich) (Table I) for 1 h at room temperature. Staining was detected using chemical luminescence methodology (GE Healthcare). The intensity of STAT1, phospho-STAT1, and actin were calculated using an image analyzing system (National Institutes of Health, ImageJ). STAT1 was normalized to actin, and the values were divided by the values at time 0 to calculate the fold induction of STAT1. Furthermore, phospho-STAT1 was normalized to STAT1.

Quantitative real-time PCR

Mice were deeply anesthetized, perfused transcardially with 20 ml cold PBS, and the brains were removed. The hippocampi from the contralateral and lesioned hemispheres were dissected out, snap frozen in liquid nitrogen, and stored at −80°C for RNA extraction.

Total RNA was isolated using TRIzol (Invitrogen) according to the manufacturer's protocol for whole-tissue RNA extraction, and then diluted in 30 μl RNase-free water.

Residual DNA was removed by treatment with 1 U DNase per 1 μg RNA (RQ1 RNase-free DNase, Promega) at 37°C for 30 min. For reverse transcription to generate cDNA, RNA was incubated with Moloney murine leukemia virus reverse transcriptase (Invitrogen), according to the manufacturer's protocol, using random hexamer primers (Invitrogen).

Quantitative real-time PCR was performed using an ABI Prism 7300 sequence detection system (Applied Biosystems) (31, 32). 18S ribosomal RNA was measured as a control and used to normalize gene expression (Applied Biosystems). Each reaction was performed in 25 μl total volume using TaqMan Reverse Universal PCR Master Mix (Applied Biosystems) containing a mixture of forward and reverse oligonucleotide primers and a specific TaqMan probe.

Primer and probe sequences were as follows: STAT2: forward, GCATTT GGCTACCTGGATTGA,reverse,GGCCTTGGCGTCATCACT,probe,FAM-AGACCAGAACTGGAGGGA-MGB; CCL2: forward, TCTGGGCCT GCT GTTCACA, reverse, CCTACTCATTGGGATCATCTTGCT, probe, FAM-CTCAGCCAGATGCAGTT-MGB. Conditions for the PCR were 2 min at 50°C, 10 min at 95°C, and then 40 cycles, each consisting of 15 s at 95°C and 1 min at 60°C. To determine the relative RNA levels within the samples, standard curves for the PCR were prepared by serial dilutions of a reference

[3] Abbreviations used in this paper: WT, wild type; dpl, days postlesion; GFAP, glial fibrillary acidic protein; PBST, PBS containing 0.5% Triton X-100.

cDNA sample. The relative expression level for each sample was calculated by dividing the expression level of the target gene by the expression level of 18S rRNA (32).

Flow cytometry

Mice were deeply anesthetized and perfused transcardially with cold PBS. The brains were removed and contralateral and lesion-reactive hippocampi were dissected out and homogenized through a 70-μm cell strainer (BD Falcon) in HBSS (Invitrogen). To block nonspecific staining, homogenates were incubated with blocking solution containing FACS buffer (2% FBS (Invitrogen), 0.1% sodium azide, HBSS) containing anti-FcIII/II receptor Ab (BD Biosciences) and Syrian hamster Ig (Jackson ImmunoResearch Laboratories) for 45 min at 4°C. Cells were stained with PE-conjugated anti-CD45, PerCP-conjugated anti-CD11b, and allophycocyanin-conjugated anti-TCRβ Abs (BD Biosciences) to detect microglia/macrophages or T cells, respectively (10, 23). Data were collected on a FACSCalibur (BD Biosciences) and analyzed using FlowJo software (Tree Star).

Statistical analysis

Results were analyzed by a two-tailed unpaired *t* test or one-way ANOVA with Bonferroni's post test using the GraphPad Prism software. A *p*-value of <0.05 was considered to be statistically significant.

Results

Up-regulation of STAT2 by glial cells in response to axotomy

To examine glial cell signaling following axonal injury, we focused our attention to the outer molecular layer of the dentate gyrus since this is where the lesion-reactive glial response is known to occur (21). We studied STAT expression within 1–5 days postlesion (dpl), since emerging and full-blown microglial and astrocyte responses occur in this period of time (25, 29, 33). Immunoreactivity for STAT2 in this region was weak in unmanipulated mice and in the contralateral hippocampus after axotomy, and it was confined to rare dispersed cells (Fig. 1, *A* and *B*, arrows). However, in the denervated, lesion-reactive (ipsilateral) hippocampus, STAT2 immunoreactivity became much stronger and the number of positively stained cells greatly increased after axotomy (Fig. 1*C*, black arrows). Increased STAT2 immunoreactivity was initially observed in glial cells at 3 dpl (not shown). STAT2 immunoreactivity was markedly increased at 5 days. At these time points, the border separating intense STAT2 labeling in the outer molecular layer from the relatively immunonegative inner molecular layer could easily be discerned (Fig. 1*C*, white arrows). Cells expressing STAT2 had a stellate morphology (Fig. 1*D*, arrows).

The absence of STAT2 immunoreactivity in sections from the lesion-reactive hippocampus of STAT2-deficient mice at 5 days (Fig. 1*E*) and lack of staining with control rabbit IgG at 5 days (Fig. 1*F*) supported specificity of STAT2 staining. We also tested the specificity of the Ab by Western blotting. STAT2 protein was present at low intensity in lysates of hippocampi from WT mice but was not detected in STAT2-deficient mice (Fig. 1*G*). Additionally, hippocampal extracts from WT mice showed increased levels of STAT2 at 5 dpl (Fig. 1*G*).

Axonal lesions induced increased STAT2 gene expression

Increased expression of STAT2 could also be shown at the level of mRNA. STAT2 mRNA was constitutively expressed in the unlesioned hippocampus (Fig. 2). After entorhinal axotomy, levels of mRNA for STAT2 increased (Fig. 2). Increased STAT2 mRNA levels relative to the unmanipulated hippocampus were detectable in the lesion-reactive hippocampus at 1 dpl, and these increases were sustained through 2 and 5 days (Fig. 2).

STAT1 and STAT2 were expressed by astrocytes

The cellular expression of STAT2 was examined by double immunofluorescence staining. Double labeling with Mac-1/CD11b

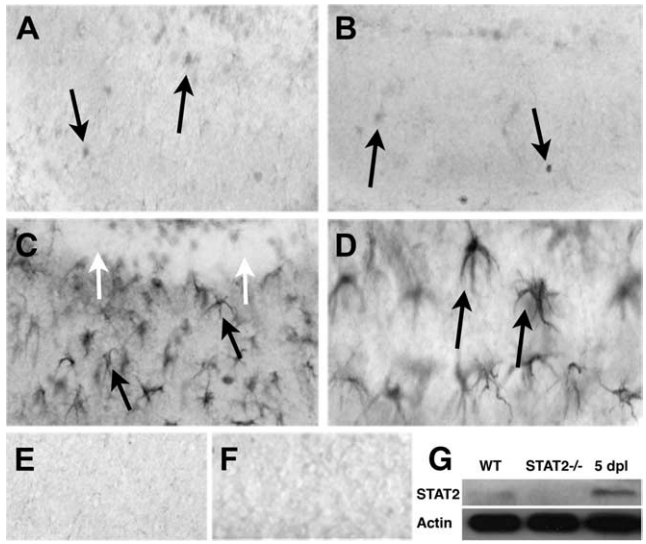

FIGURE 1. STAT2 immunoreactivity in the outer molecular layer of dentate gyrus after axonal injury. Very few weakly stained STAT2-positive cells were detected in unmanipulated mice (*A*, arrows) and in the contralateral hippocampus after lesion at 5 days (*B*, arrows). Five days after lesion, STAT2 immunoreactivity was markedly increased in the dentate gyrus ipsilateral to lesion (*C*, black arrows). Arrows indicate the relatively immunonegative inner molecular layer (*C*, white arrows). Higher magnification of STAT2-immunopositive cells (*D*, arrows). STAT2 immunoreactivity was localized to cell bodies and processes of cells with stellate morphology (*D*, arrows). STAT2 staining was not detected in lesion-reactive hippocampus from STAT2-deficient mice at 5 days (*E*). Control sections from lesion-reactive hippocampus at 5 days stained with rabbit IgG showed no immunoreactivity (*F*). *G*, Western blot for STAT2 protein in hippocampal extracts from unmanipulated WT mice, showing that levels increased at 5 dpl, and that STAT2 protein was not detectable in unmanipulated STAT2$^{-/-}$ mice. Original magnifications $\times$20 (*A–C*, *E*, and *F*), $\times$100 (*D*).

(microglia/macrophages) and GFAP (astrocytes) showed that STAT2 colocalized exclusively with astrocytes (Fig. 3, *D–F*) and not with microglia (Fig. 3, *A–C*).

When activated, STATs become phosphorylated and dimerize. Activated STAT2 associates with activated STAT1 to form a heterodimer, which is required for the activation of transcription (34).

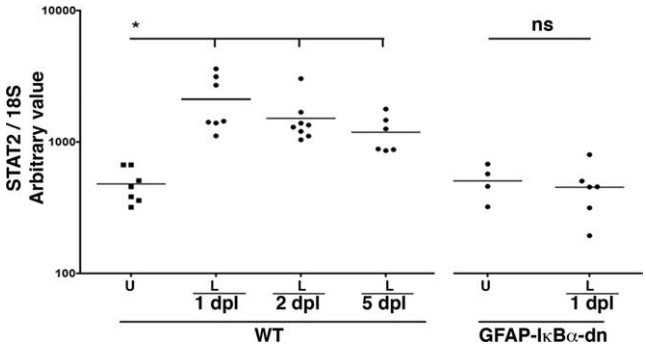

FIGURE 2. STAT2 gene expression in hippocampus after axonal lesion. Quantitative real-time PCR shows that STAT2 mRNA was expressed at low levels in the unmanipulated hippocampus from WT ($n = 7$) and GFAP-IκBα-dn mice ($n = 4$). In WT mice, following entorhinal lesion, the expression of message for STAT2 was significantly increased in lesion-reactive hippocampi at 1 ($n = 7$), 2 ($n = 8$), and 5 days ($n = 6$). Compared with unmanipulated hippocampi ($n = 4$), STAT2 mRNA remained unchanged in lesion-reactive hippocampi ($n = 6$) of GFAP-IκBα-dn mice. U indicates unmanipulated; L, lesion-reactive hippocampi.

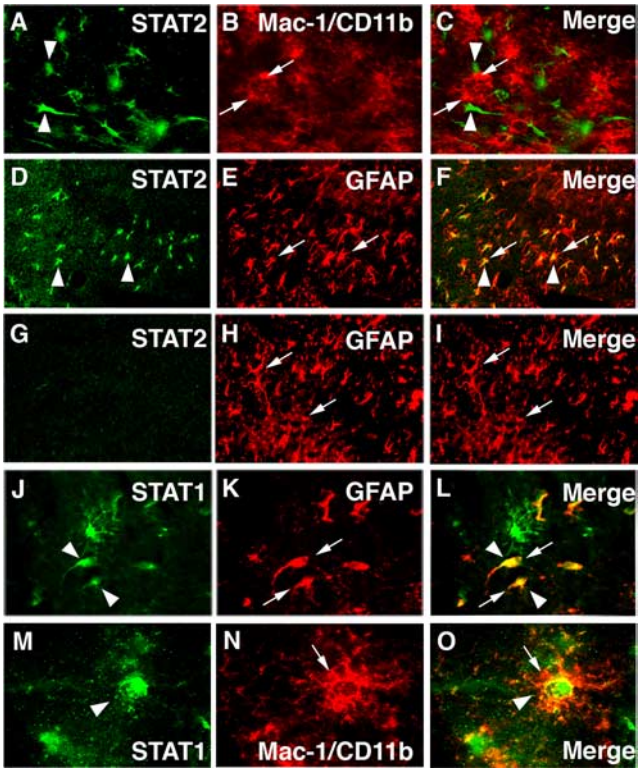

FIGURE 3. Cellular localization of STAT1 and STAT2 in the outer molecular layer of dentate gyrus ipsilateral to lesion. *A–F*, Immunofluorescent visualization of cells expressing STAT2 (*A* and *D*, green, arrowheads), Mac-1/CD11b (*B*, red, arrows), and GFAP (*E*, red, arrow) at 5 dpl in WT mice. STAT2 did not colocalize with Mac-1/CD11b (*C*). *F*, Dual labeling shows STAT2 overlap (yellow) with GFAP demonstrating the association of STAT2 with astrocytes. STAT2 immunoreactivity was not observed in lesion-reactive hippocampus of GFAP-IκBα-dn mice at 5 days after axonal lesion (*G* and *I*). Inactivation of NF-κB in astrocytes had no effect on GFAP immunoreactivity (*H*). *L*, Dual labeling (yellow) shows colocalization of STAT1 (*J*, green, arrowheads) with GFAP (*K*, red, arrows) at 5 dpl in WT mice. The large GFAP-negative cell (green) in *L* shows microglial morphology. *O*, Dual labeling shows colocalization of STAT1 (*M*, green, arrowhead) with Mac-1/CD11b (*N*, red, arrow). Original magnification ×40 (*D–I*), ×80 (*A–C*, *J–L*), and ×200 (*M–O*).

We examined if STAT1 is expressed in astrocytes as well as STAT2. Indeed, STAT1 was up-regulated in lesion-reactive hippocampus (see Fig. 5*D*) and colocalized with both microglia (Fig. 3*M–O*) and astrocytes at 5 days after axonal lesion (Fig. 3*J–L*).

Detection of phospho-STAT2

Phosphorylation of STAT2 indicates its involvement in active signaling (34). Due to antibody-related technical reasons, we are unable to detect phospho-STAT2 by Western blot. However, we could detect phospho-STAT2 by immunostaining. Phospho-STAT2 immunostaining was observed as early as 1 day (Fig. 4, *A* and *B*) and was detectable at 3 and 5 days (Fig. 4*C–F* and not shown). This staining was not detected in denervated hippocampus from STAT2-deficient mice (Fig. 4*A*, *insert*). Like STAT2 staining, phospho-STAT2 staining colocalized with astrocytes and was exclusively localized to nuclei (Fig. 4*C–F*). For technical reasons, we are unable to detect phospho-STAT1 by immunohistochemistry, but using Western blot we could show STAT1 phosphorylation in lesion-reactive hippocampi at 1, 3, and 5 days after axonal injury (Fig. 5*A*). Taken together, these data suggest that phosphorylated STAT1/2 heterodimers are activated in astrocytes in response to injury-associated signals.

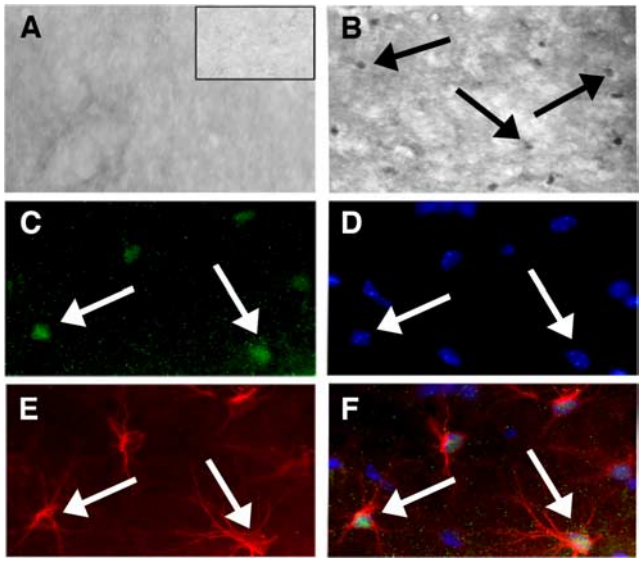

FIGURE 4. STAT2 phosphorylation in response to axonal lesion. *A*, Phospho-STAT2 immunostaining was undetectable in the contralateral dentate gyrus at 1 day. *B*, Phospho-STAT2 staining (arrows) become detectable in the outer molecular layer ipsilateral to the lesion at 1 day. Phospho-STAT2 staining was not detected in lesion-reactive hippocampus from STAT2-deficient mice at 1 day (*A*, insert). *C–F*, Immunofluorescent visualization of cells expressing (*C*) phospho-STAT2 (green, arrows), (*D*) DAPI (blue, arrows), and (*E*) GFAP (red, arrows). Triple-labeling shows phospho-STAT2 overlap with DAPI in GFAP-positive cells, demonstrating nuclear localization of phospho-STAT2 in astrocytes (*F*). Original magnification ×20 (*A*) and ×80 (*B–F*).

STAT2 up-regulation in astrocytes was NF-κB dependent

The selective activation and colocalization of STAT2 in astrocytes, together with the fact that NF-κB signaling is involved in the control of a number of responses during inflammation, raised the question of whether STAT2 expression in astrocytes is controlled by NF-κB signaling. We took advantage of GFAP-IκBα-dn mice, in which NF-κB activation in astrocytes is disabled by expression

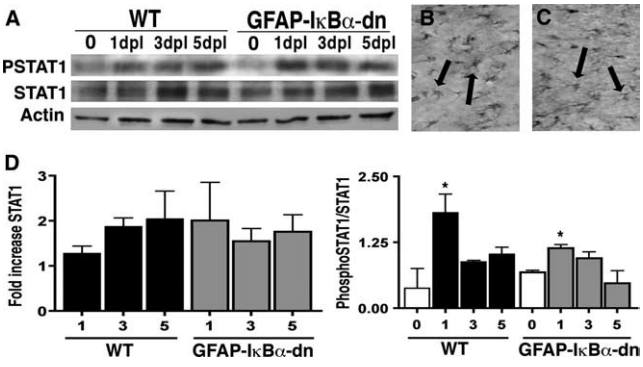

FIGURE 5. STAT1 and phospho-STAT1 up-regulation in response to axonal lesion. *A*, Western blot analysis of hippocampal extracts showing up-regulation of phospho-STAT1 (PSTAT1) and STAT1 at 1, 3, and 5 dpl in WT (*lanes 1–4*) and GFAP-IκBα-dn mice (*lanes 5–8*) in comparison to the respective unmanipulated mice. *B* and *C*, STAT1 immunostaining was observed in glial cells in lesion-reactive hippocampus of WT (*B*) and GFAP-IκBα-dn mice (*C*). Arrows indicate examples of STAT1-immunostained cells in the lesion-reactive hippocampus of WT (*B*) and GFAP-IκBα-dn mice (*C*). *D*, Western blot analysis of hippocampal extracts showing kinetics of up-regulation of STAT1 (*left panel*) and phospho-STAT1 (*right panel*) in WT and GFAP-IκBα-dn mice. Original magnifications ×8 (*B* and *C*).

of a dominant-negative IκBα construct (19). Lesion-induced increases in GFAP and Mac-1/CD11b levels were not affected in these mice (Fig. 3*H* and data not shown). GFAP-IκBα-dn mice displayed no increase in STAT2 immunoreactivity (Fig. 3*G–I*) after axotomy. Additionally, the level of STAT2 mRNA in lesion-reactive hippocampi that was measured by quantitative real-time PCR mRNA was unchanged in comparison to unmanipulated GFAP-IκBα-dn mice (Fig. 2). Phospho-STAT2 staining was not detectable in the hippocampi of GFAP-IκBα-dn mice after axonal injury (not shown). Taken together, these findings indicate that injury-driven STAT2 up-regulation and activation in astrocytes was NF-κB-dependent. Interestingly, up-regulation and kinetics of both STAT1 and phospho-STAT1 were equivalent in WT and GFAP-IκBα-dn (Fig. 5*D*). This could be shown by Western blot (Fig. 5, *A* and *D*) as well as by immunohistochemistry for STAT1 (Fig. 5, *B* and *C*). STAT1-positive cells in Fig. 5, *B* and *C*, were identifiable by morphology as including both astrocytes and microglia, but this was not examined further.

Inhibition of astroglial NF-κB signaling reduced CCL2 gene expression and leukocyte infiltration

Chemokine production is an important response to injury, especially CCL2, which we have shown to be produced by microglia and astrocytes and to be necessary for recruitment of leukocytes to the injury-reactive hippocampus (10). CCL2 message was transcribed by astrocytes and microglia in response to injury, but the relative contribution of each glial cell type in recruiting leukocytes was not shown (10). The GFAP-IκBα-dn mice allowed us to examine the role of NF-κB in the injury-driven CCL2 response in astrocytes, as well as the functional significance of NF-κB-signaled astrocyte response. CCL2 mRNA was constitutively expressed at a low level, equivalent in both mice, in the unlesioned hippocampus of WT (C57BL/6) and GFAP-IκBα-dn mice (not shown). CCL2 mRNA was significantly increased after axotomy in both WT and GFAP-IκBα-dn mice (Fig. 6*A*). However, the level of CCL2 mRNA in lesion-reactive hippocampi from GFAP-IκBα-dn mice was ~50% of, and significantly lower than, levels in WT mice (Fig. 6*A*). This suggests that NF-κB is a critical signal for injury-induced CCL2 transcription in astrocytes, and that this astrocyte response contributes about half of the hippocampal CCL2 response. To investigate the functional significance of astroglial NF-κB-signaled CCL2 production, we compared infiltration of leukocytes (which included both macrophages and T cells (10, 23, 35)) to the injury-reactive hippocampus in WT and GFAP-IκBα-dn mice (Fig. 6, *B* and *C*). Proportions of blood-derived leukocytes (defined as $CD45^{high}$ cells by FACS to exclude CNS-resident microglia (35, 36)) were similarly low in unmanipulated hippocampi from WT and GFAP-IκBα-dn mice (not shown). The proportion of $CD45^{high}$ cells was significantly increased in the lesion-reactive hippocampi of both WT and GFAP-IκBα-dn mice compared with the contralateral hippocampus of each mouse (Fig. 6, *B* and *C*). However, as for CCL2 mRNA, the proportions of infiltrating $CD45^{high}$ cells were ~50% of, and significantly lower in, GFAP-IκBα-dn than in WT mice (Fig. 6, *B* and *C*). The relative proportion of macrophages and T cells within the $CD45^{high}$ population did not change in GFAP-IκBα-dn mice.

As expected, NF-κB inactivation in astrocytes had no effect on microglia. There was no significant difference between the proportions of $CD11b^{+}CD45^{dim}$ microglia in lesion-reactive hippocampi of WT and GFAP-IκBα-dn mice (not shown).

CCL2 gene expression in STAT2- and STAT1-deficient mice

The inactivation of NF-κB signaling in astrocytes resulted in 50% reduction of both CCL2 gene expression and leukocyte infiltration

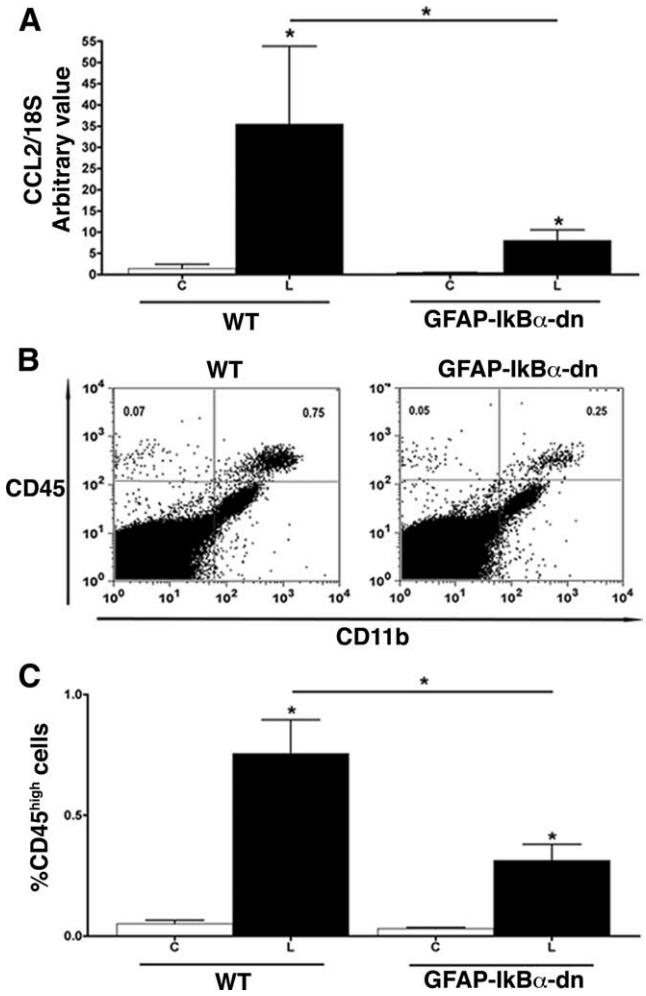

FIGURE 6. The prevention of NF-κB activation in astrocytes resulted in reduction in both level of CCL2 mRNA and leukocyte infiltration. Levels of CCL2 mRNA, measured by quantitative real-time PCR, were significantly increased in lesion-reactive hippocampi from both WT (C57BL/6) ($n = 6$) and GFAP-IκBα-dn mice ($n = 6$) compared with contralateral hippocampi at 1 day (*A*). However, lesion-induced CCL2 mRNA levels were significantly lower in GFAP-IκBα-dn mice than in WT mice. The functional significance of NF-κB-signaled CCL2 expression was examined by flow cytometry (*B* and *C*). *B*, Shown are representative double-staining profiles for CD11b and CD45 of lesion-reactive hippocampi from WT (*left panel*) and GFAP-IκBα-dn mice (*right panel*) at 1 day after axonal lesion. Proportions of infiltrating $CD45^{high}$ cells were significantly increased in lesion-reactive hippocampi of both WT ($n = 6$) and GFAP-IκBα-dn mice ($n = 7$) compared with contralateral (quantitations in *C*). However, the proportion of $CD45^{high}$ cells in lesion-reactive hippocampi of GFAP-IκBα-dn mice was significantly lower than in the WT mice (*C*). C indicates contralateral; L, lesion-reactive hippocampi.

in response to injury. STAT2 up-regulation in astrocytes was also NF-κB-dependent. We then examined the effect of STAT1 and STAT2 deficiency on the injury-induced inflammatory response. There was no difference in basal CCL2 mRNA levels in hippocampi of WT (129s6/SvEv), STAT1-deficient, and STAT2-deficient mice (not shown). As for GFAP-IκBα-dn mice, injury-induced increases in levels of GFAP and Mac-1/CD11b were not affected in these mice (not shown). As has been previously shown for C57BL/6 mice (Ref. 10 and Fig. 6*A*), CCL2 mRNA expression increased significantly in lesion-reactive hippocampi of 129s6/SvEv mice (Fig. 7). Notably, lesion-induced increases in CCL2 mRNA levels in hippocampi of STAT1- and STAT2-deficient

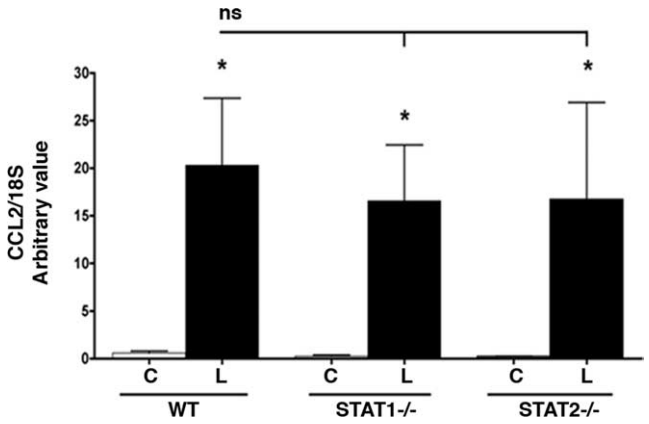

FIGURE 7. Lack of STAT1 and STAT2 had no effect on CCL2 gene expression. CCL2 mRNA was significantly increased in lesion-reactive hippocampi of WT (129s6/SvEv) ($n = 6$), STAT1-deficient ($n = 6$), and STAT2-deficient ($n = 6$) mice compared with contralateral at 1 day after axonal lesion. In the lesion-reactive hippocampi no statistically significant differences could be measured between the WT, STAT1-deficient, and STAT2-deficient mice, indicating that STAT1 and STAT2 had no effect on CCL2 gene expression. ns indicates not significant; C, contralateral; L, lesion-reactive hippocampi.

mice were equivalent to those in WT mice (Fig. 7). These results indicate that whereas both the induction of STAT2 and the CCL2 message are dependent on NF-κB signaling, the CCL2 response is independent of either STAT1 or STAT2.

Discussion

Injury-induced inflammation includes expression of genes encoding cytokines and chemokines that regulate the infiltration of immune cells into the injury-reactive tissue. We have studied STAT and CCL2 regulation and their relationship to NF-κB signaling in a model of glial and leukocyte response to axonal transection in the CNS. We show that these injury-induced signals include activation of receptor-associated transcription factors including STATs and NF-κB. We show that STAT2 is activated and up-regulated exclusively in astrocytes in the hippocampus in response to axotomy, and that this is entirely dependent on NF-κB. We further show that astrocytes contribute 50% of the injury-induced CCL2 response, and that this and the leukocyte infiltration that it is known to direct are also dependent on NF-κB.

STAT2 activation and up-regulation in astrocytes in response to injury have not previously been reported. STAT2 signaling is known to play a critical role in antiviral defense mechanisms in the CNS (37). A number of studies have investigated the expression and regulation of STAT2 in other models of CNS inflammation. Up-regulation of STAT2 in experimental autoimmune encephalomyelitis has been demonstrated (38). Lack of STAT2 in transgenic mice with astrocyte production of IFN-α resulted in the development of medulloblastoma and their early death (39). Our findings now extend the involvement of STAT2 responses to axonal injury and suggest that STAT2 activators act selectively on injury-reactive astrocytes.

Activation of STAT2 leads to its dimerization, classically with STAT1, to form a complex that induces gene transcription (34). We found that STAT1 was also up-regulated in response to injury, not only in astrocytes, but also in microglia, and we show that STAT1 was also phosphorylated. STAT1 phosphorylation was evident in both WT and GFAP-IκBα-dn mice, indicating active STAT1 signaling. Although we are not able to show the cellular localization of phospho-STAT1 in lesion-reactive hippocampi, it is likely that both astrocytes and microglia contributed to this observation in WT mice, since STAT1 immunoreactivity has been observed in both microglia (Mac-1/CD11b$^+$) and astroglial (GFAP$^+$) cells. Whether STAT1 is activated independently of STAT2 in GFAP-IκBα-dn mice or whether the Western blot signal that we detect reflects expression by other cells cannot be determined at this time. Our findings therefore indicate active STAT1/2 signaling in astrocytes. Hua et al. (40) have shown the induction of mRNA and protein for STAT1 and STAT2 in isolated human astrocytes in response to IFNs, which are classically implicated in antiviral responses, and may be speculated to play a role in response to injury. In primary astrocytes, Qin et al. (41) showed that IL-27 induces expression of an inhibitor of the STAT signaling pathway, the suppressor of cytokine signaling. We do not think that exclusive STAT2 activation in astrocytes reflects inability of microglia to express STAT2, since preliminary results show STAT2 mRNA expression in both microglia and astrocytes sorted from normal CNS (T. Holm and R. Khorooshi, unpublished). The up-regulation of STAT2 exclusively in astrocytes in the lesion-reactive hippocampus more likely indicates their selective responsiveness to STAT2-signaling receptor. Astrocytes respond to a number of stimuli with increases in expression of inflammatory mediators (40, 42–45), and it is possible that such inflammatory signals contributed to microglial response (1). However, Mac-1/CD11b (microglial) and GFAP (astroglial) immunoreactivity were unaffected in lesion-reactive hippocampi from STAT1- and STAT2-deficient mice compared with WT mice. Our results also showed that CCL2 expression is independent of either STAT2 or STAT1.

Interestingly, STAT2 activation in astrocytes was prevented in GFAP-IκBα-dn mice. Regulation of STAT2 is a novel finding that adds to interest in NF-κB as a mediator of glial response (17, 19). In contrast to CCL2, whose promoter region contains recognition sites for NF-κB (46), the mechanism by which NF-κB regulates STAT2 up-regulation and activation is not known. Whether the STAT2 promoter contains a binding site for NF-κB has not been shown. Regulation by NF-κB could also be indirect. NF-κB complexes are involved in the control of a number of cellular responses during inflammatory and degenerative responses, and NF-κB signaling regulates the transcription of a variety of genes that play potential roles in inflammatory reactions and neuronal survival after injury (19, 47–49). We further showed that inhibition of NF-κB activation resulted in a significant reduction (~50%) of CCL2 gene expression in lesion-reactive hippocampi. Reduced CCL2 gene expression was also reported in GFAP-IκBα-dn mice after spinal cord injury (19). This NF-κB dependence was selective since it did not affect GFAP expression, as has been shown previously (19).

We had previously shown that both astrocytes and microglia were induced to express CCL2 mRNA by entorhinal axotomy, and that proportions of these CCL2-positive cells were similar (10). Our finding that NF-κB inactivation in astrocytes reduced hippocampal CCL2 levels to 50% is most directly consistent with the interpretation that the astrocyte-signaled fraction of the CCL2 response is dependent on NF-κB signaling. Our data do not exclude that NF-κB inhibition in astrocytes indirectly led to reduction of CCL2 production via inhibition of some intermediate pathway that then acted either autocrine on astrocytes themselves or paracrine on other cells. Regardless of whether the mechanism was via direct production or indirect regulation, our findings show that the astrocyte contribution to injury-induced CCL2 expression was NF-κB controlled and matched the aggregate from microglia and other CCL2-expressing cells, which potentially can include neurons, endothelial cells, and leukocytes (10). This was supported by the

finding that leukocyte infiltration into the lesion-reactive hippocampus was comparably reduced (50%) in GFAP-IκBα-dn mice. We have previously shown that CCL2, acting through CCR2, is essential for leukocyte infiltration in this model, so the two observations are functionally linked. Consistent with this, it has been reported that experimental autoimmune encephalomyelitis was milder and leukocyte infiltration to CNS reduced in mice with defective NF-κB signaling in cells that included neurons, oligodendrocytes, and astrocytes (50).

Infiltrating macrophages and T cells are variously reported to be harmful or of benefit in CNS injury responses (51, 52). Macrophage infiltration into the injured CNS promotes repair (53). Several studies have investigated subsets of T cells infiltrating the injured CNS. In response to peripheral nerve injury, $CD4^+$ Th2 cells that infiltrate the facial nucleus promoted the survival of facial motor neurons (54–56). Consistent with a role for Th2 T cells, message for IFN-γ, a Th1 cytokine, was undetectable in hippocampus in response to axonal lesion (57). Recruitment of both $CD4^+$ and $CD8^+$ cells to the demyelinated corpus callosum has been demonstrated (58), and our recent studies described infiltration of $CD3^+CD45^{high}$ T cells into the lesion-reactive hippocampus (10, 23). Our current findings indicate that astrocytes make a significant contribution to the recruitment of immune cells into the injured brain, giving astrocytes a central role in the maintenance of CNS homeostasis. The astrocyte response to axonal injury involves STAT2 signaling, which is dependent on NF-κB. Additionally, NF-κB signaling in astrocytes controls both CCL2 expression and leukocyte infiltration into lesion-reactive hippocampus after axonal injury. These findings together extend our appreciation of, and indicate a central role for, astrocytes in the maintenance of CNS homeostasis.

Acknowledgments

We thank Pia Nyborg Nielsen and Dina Draeby for excellent technical support and Mie Rytz Hansen for help with Western blots. We also thank Jason Millward for constructive comments. We thank Dr. Chris Schindler (Columbia University, New York, NY) for providing the STAT2-deficient mice and Dr. John R. Bethea (Miller School of Medicine, University of Miami, FL) for providing the GFAP-IκBα-dn mice.

Disclosures

The authors have no financial conflicts of interest.

References

1. Farina, C., F. Aloisi, and E. Meinl. 2007. Astrocytes are active players in cerebral innate immunity. *Trends Immunol.* 28: 138–145.
2. Hanisch, U. K., and H. Kettenmann. 2007. Microglia: active sensor and versatile effector cells in the normal and pathologic brain. *Nat. Neurosci.* 10: 1387–1394.
3. Prat, A., K. Biernacki, K. Wosik, and J. P. Antel. 2001. Glial cell influence on the human blood-brain barrier. *Glia* 36: 145–155.
4. Dong, Y., and E. N. Benveniste. 2001. Immune function of astrocytes. *Glia* 36: 180–190.
5. Minagar, A., P. Shapshak, R. Fujimura, R. Ownby, M. Heyes, and C. Eisdorfer. 2002. The role of macrophage/microglia and astrocytes in the pathogenesis of three neurologic disorders: HIV-associated dementia, Alzheimer disease, and multiple sclerosis. *J. Neurol. Sci.* 202: 13–23.
6. Ambrosini, E., and F. Aloisi. 2004. Chemokines and glial cells: a complex network in the central nervous system. *Neurochem. Res.* 29: 1017–1038.
7. Owens, T., A. A. Babcock, J. M. Millward, and H. Toft-Hansen. 2005. Cytokine and chemokine inter-regulation in the inflamed or injured CNS. *Brain Res. Brain Res. Rev.* 48: 178–184.
8. Huang, D., Y. Han, M. R. Rani, A. Glabinski, C. Trebst, T. Sorensen, M. Tani, J. Wang, P. Chien, S. O'Bryan, et al. 2000. Chemokines and chemokine receptors in inflammation of the nervous system: manifold roles and exquisite regulation. *Immunol. Rev.* 177: 52–67.
9. Ransohoff, R. M. 2002. The chemokine system in neuroinflammation: an update. *J. Infect. Dis.* 186 (*Suppl.* 2): S152–S156.
10. Babcock, A. A., W. A. Kuziel, S. Rivest, and T. Owens. 2003. Chemokine expression by glial cells directs leukocytes to sites of axonal injury in the CNS. *J. Neurosci.* 23: 7922–7930.
11. Thibeault, I., N. Laflamme, and S. Rivest. 2001. Regulation of the gene encoding the monocyte chemoattractant protein 1 (MCP-1) in the mouse and rat brain in response to circulating LPS and proinflammatory cytokines. *J. Comp. Neurol.* 434: 461–477.
12. Flugel, A., G. Hager, A. Horvat, C. Spitzer, G. M. Singer, M. B. Graeber, G. W. Kreutzberg, and F. W. Schwaiger. 2001. Neuronal MCP-1 expression in response to remote nerve injury. *J. Cereb. Blood Flow Metab.* 21: 69–76.
13. Martin, T., P. M. Cardarelli, G. C. Parry, K. A. Felts, and R. R. Cobb. 1997. Cytokine induction of monocyte chemoattractant protein-1 gene expression in human endothelial cells depends on the cooperative action of NF-κB and AP-1. *Eur. J. Immunol.* 27: 1091–1097.
14. Kim, J. M., Y. K. Oh, J. H. Lee, D. Y. Im, Y. J. Kim, J. Youn, C. H. Lee, H. Son, Y. S. Lee, J. Y. Park, and I. H. Choi. 2005. Induction of proinflammatory mediators requires activation of the TRAF, NIK, IKK and NF-κB signal transduction pathway in astrocytes infected with *Escherichia coli*. *Clin. Exp. Immunol.* 140: 450–460.
15. Lawrence, D. M., P. Seth, L. Durham, F. Diaz, R. Boursiquot, R. M. Ransohoff, and E. O. Major. 2006. Astrocyte differentiation selectively upregulates CCL2/monocyte chemoattractant protein-1 in cultured human brain-derived progenitor cells. *Glia* 53: 81–91.
16. Ohmori, Y., and T. A. Hamilton. 1995. The interferon-stimulated response element and a κB site mediate synergistic induction of murine IP-10 gene transcription by IFN-gamma and TNF-alpha. *J. Immunol.* 154: 5235–5244.
17. Bethea, J. R., M. Castro, R. W. Keane, T. T. Lee, W. D. Dietrich, and R. P. Yezierski. 1998. Traumatic spinal cord injury induces nuclear factor-κB activation. *J. Neurosci.* 18: 3251–3260.
18. Pollock, G., K. R. Pennypacker, S. Memet, A. Israel, and S. Saporta. 2005. Activation of NF-κB in the mouse spinal cord following sciatic nerve transection. *Exp. Brain Res.* 165: 470–477.
19. Brambilla, R., V. Bracchi-Ricard, W. H. Hu, B. Frydel, A. Bramwell, S. Karmally, E. J. Green, and J. R. Bethea. 2005. Inhibition of astroglial nuclear factor κB reduces inflammation and improves functional recovery after spinal cord injury. *J. Exp. Med.* 202: 145–156.
20. Ousman, S. S., J. Wang, and I. L. Campbell. 2005. Differential regulation of interferon regulatory factor (IRF)-7 and IRF-9 gene expression in the central nervous system during viral infection. *J. Virol.* 79: 7514–7527.
21. Finsen, B., M. B. Jensen, N. D. Lomholt, I. V. Hegelund, F. R. Poulsen, and T. Owens. 1999. Axotomy-induced glial reactions in normal and cytokine transgenic mice. *Adv. Exp. Med. Biol.* 468: 157–171.
22. Ladeby, R., M. Wirenfeldt, I. Dalmau, R. Gregersen, D. Garcia-Ovejero, A. Babcock, T. Owens, and B. Finsen. 2005. Proliferating resident microglia express the stem cell antigen CD34 in response to acute neural injury. *Glia* 50: 121–131.
23. Babcock, A. A., M. Wirenfeldt, T. Holm, H. H. Nielsen, L. Dissing-Olesen, H. Toft-Hansen, J. M. Millward, R. Landmann, S. Rivest, B. Finsen, and T. Owens. 2006. Toll-like receptor 2 signaling in response to brain injury: an innate bridge to neuroinflammation. *J. Neurosci.* 26: 12826–12837.
24. Wirenfeldt, M., L. Dissing-Olesen, A. Anne Babcock, M. Nielsen, M. Meldgaard, J. Zimmer, I. Azcoitia, R. G. Leslie, F. Dagnaes-Hansen, and B. Finsen. 2007. Population control of resident and immigrant microglia by mitosis and apoptosis. *Am. J. Pathol.* 171: 617–631.
25. Fagan, A. M., and F. H. Gage. 1994. Mechanisms of sprouting in the adult central nervous system: cellular responses in areas of terminal degeneration and reinnervation in the rat hippocampus. *Neuroscience* 58: 705–725.
26. Frotscher, M., B. Heimrich, and T. Deller. 1997. Sprouting in the hippocampus is layer-specific. *Trends Neurosci.* 20: 218–223.
27. Meraz, M. A., J. M. White, K. C. Sheehan, E. A. Bach, S. J. Rodig, A. S. Dighe, D. H. Kaplan, J. K. Riley, A. C. Greenlund, D. Campbell, et al. 1996. Targeted disruption of the Stat1 gene in mice reveals unexpected physiologic specificity in the JAK-STAT signaling pathway. *Cell* 84: 431–442.
28. Park, C., S. Li, E. Cha, and C. Schindler. 2000. Immune response in Stat2 knockout mice. *Immunity* 13: 795–804.
29. Jensen, M. B., I. V. Hegelund, F. R. Poulsen, T. Owens, J. Zimmer, and B. Finsen. 1999. Microglial reactivity correlates to the density and the myelination of the anterogradely degenerating axons and terminals following perforant path denervation of the mouse fascia dentata. *Neuroscience* 93: 507–518.
30. Munzberg, H., L. Huo, E. A. Nillni, A. N. Hollenberg, and C. Bjorbaek. 2003. Role of signal transducer and activator of transcription 3 in regulation of hypothalamic proopiomelanocortin gene expression by leptin. *Endocrinology* 144: 2121–2131.
31. Toft-Hansen, H., R. K. Nuttall, D. R. Edwards, and T. Owens. 2004. Key metalloproteinases are expressed by specific cell types in experimental autoimmune encephalomyelitis. *J. Immunol.* 173: 5209–5218.
32. Toft-Hansen, H., A. A. Babcock, J. M. Millward, and T. Owens. 2007. Down-regulation of membrane type-matrix metalloproteinases in the inflamed or injured central nervous system. *J. Neuroinflamm.* 4: 24.
33. Deller, T., M. Frotscher, and R. Nitsch. 1996. Sprouting of crossed entorhinodentate fibers after a unilateral entorhinal lesion: anterograde tracing of fiber reorganization with *Phaseolus vulgaris*-leucoagglutinin (PHAL). *J. Comp. Neurol.* 365: 42–55.
34. Schindler, C., D. E. Levy, and T. Decker. 2007. JAK-STAT signaling: from interferons to cytokines. *J. Biol. Chem.* 282: 20059–20063.
35. Sedgwick, J. D., S. Schwender, H. Imrich, R. Dorries, G. W. Butcher, and V. ter Meulen. 1991. Isolation and direct characterization of resident microglial cells from the normal and inflamed central nervous system. *Proc. Natl. Acad. Sci. USA* 88: 7438–7442.
36. Renno, T., M. Krakowski, C. Piccirillo, J. Y. Lin, and T. Owens. 1995. TNF-alpha expression by resident microglia and infiltrating leukocytes in the central

nervous system of mice with experimental allergic encephalomyelitis: regulation by Th1 cytokines. *J. Immunol.* 154: 944–953.
37. Campbell, I. L. 2005. Cytokine-mediated inflammation, tumorigenesis, and disease-associated JAK/STAT/SOCS signaling circuits in the CNS. *Brain Res. Brain Res. Rev.* 48: 166–177.
38. Maier, J., C. Kincaid, A. Pagenstecher, and I. L. Campbell. 2002. Regulation of signal transducer and activator of transcription and suppressor of cytokine-signaling gene expression in the brain of mice with astrocyte-targeted production of interleukin-12 or experimental autoimmune encephalomyelitis. *Am. J. Pathol.* 160: 271–288.
39. Wang, J., N. Pham-Mitchell, C. Schindler, and I. L. Campbell. 2003. Dysregulated Sonic hedgehog signaling and medulloblastoma consequent to IFN-α-stimulated STAT2-independent production of IFN-γ in the brain. *J. Clin. Invest.* 112: 535–543.
40. Hua, L. L., M. O. Kim, C. F. Brosnan, and S. C. Lee. 2002. Modulation of astrocyte inducible nitric oxide synthase and cytokine expression by interferon β is associated with induction and inhibition of interferon γ-activated sequence binding activity. *J. Neurochem.* 83: 1120–1128.
41. Qin, H., Y. Cong, K. L. Roberts, B. J. Baker, C. O. Elson, and E. N. Benveniste. 2007. Differential regulation of SOCS gene expression by IL-27 in astrocytes and $CD4^+$ T cells. *J. Immunol.* 178: 87.11.
42. Palma, J. P., D. Kwon, N. A. Clipstone, and B. S. Kim. 2003. Infection with Theiler's murine encephalomyelitis virus directly induces proinflammatory cytokines in primary astrocytes via NF-κB activation: potential role for the initiation of demyelinating disease. *J. Virol.* 77: 6322–6331.
43. Hayashi, M., Y. Luo, J. Laning, R. M. Strieter, and M. E. Dorf. 1995. Production and function of monocyte chemoattractant protein-1 and other β-chemokines in murine glial cells. *J. Neuroimmunol.* 60: 143–150.
44. Stalder, A. K., A. Pagenstecher, N. C. Yu, C. Kincaid, C. S. Chiang, M. V. Hobbs, F. E. Bloom, and I. L. Campbell. 1997. Lipopolysaccharide-induced IL-12 expression in the central nervous system and cultured astrocytes and microglia. *J. Immunol.* 159: 1344–1351.
45. Esen, N., F. Y. Tanga, J. A. DeLeo, and T. Kielian. 2004. Toll-like receptor 2 (TLR2) mediates astrocyte activation in response to the Gram-positive bacterium *Staphylococcus aureus*. *J. Neurochem.* 88: 746–758.
46. Ueda, A., K. Okuda, S. Ohno, A. Shirai, T. Igarashi, K. Matsunaga, J. Fukushima, S. Kawamoto, Y. Ishigatsubo, and T. Okubo. 1994. NF-κB and Sp1 regulate transcription of the human monocyte chemoattractant protein-1 gene. *J. Immunol.* 153: 2052–2063.
47. Kassed, C. A., T. L. Butler, G. W. Patton, D. D. Demesquita, M. T. Navidomskis, S. Memet, A. Israel, and K. R. Pennypacker. 2004. Injury-induced NF-κB activation in the hippocampus: implications for neuronal survival. *FASEB J.* 18: 723–724.
48. Kassed, C. A., A. E. Willing, S. Garbuzova-Davis, P. R. Sanberg, and K. R. Pennypacker. 2002. Lack of NF-κB p50 exacerbates degeneration of hippocampal neurons after chemical exposure and impairs learning. *Exp. Neurol.* 176: 277–288.
49. Pennypacker, K. R., C. A. Kassed, S. Eidizadeh, S. Saporta, P. R. Sanberg, and A. E. Willing. 2001. NF-κB p50 is increased in neurons surviving hippocampal injury. *Exp. Neurol.* 172: 307–319.
50. van Loo, G., R. De Lorenzi, H. Schmidt, M. Huth, A. Mildner, M. Schmidt-Supprian, H. Lassmann, M. R. Prinz, and M. Pasparakis. 2006. Inhibition of transcription factor NF-κB in the central nervous system ameliorates autoimmune encephalomyelitis in mice. *Nat. Immunol.* 7: 954–961.
51. Jones, T. B., E. E. McDaniel, and P. G. Popovich. 2005. Inflammatory-mediated injury and repair in the traumatically injured spinal cord. *Curr. Pharm Des.* 11: 1223–1236.
52. Schwartz, M. 2003. Macrophages and microglia in central nervous system injury: are they helpful or harmful? *J. Cereb. Blood Flow Metab.* 23: 385–394.
53. Schwartz, M., G. Moalem, R. Leibowitz-Amit, and I. R. Cohen. 1999. Innate and adaptive immune responses can be beneficial for CNS repair. *Trends Neurosci.* 22: 295–299.
54. Deboy, C. A., J. Xin, S. C. Byram, C. J. Serpe, V. M. Sanders, and K. J. Jones. 2006. Immune-mediated neuroprotection of axotomized mouse facial motoneurons is dependent on the IL-4/STAT6 signaling pathway in $CD4^+$ T cells. *Exp. Neurol.* 201: 212–224.
55. Serpe, C. J., S. Coers, V. M. Sanders, and K. J. Jones. 2003. $CD4^+$ T, but not $CD8^+$ or B, lymphocytes mediate facial motoneuron survival after facial nerve transection. *Brain Behav. Immun.* 17: 393–402.
56. Raivich, G., L. L. Jones, C. U. Kloss, A. Werner, H. Neumann, and G. W. Kreutzberg. 1998. Immune surveillance in the injured nervous system: T-lymphocytes invade the axotomized mouse facial motor nucleus and aggregate around sites of neuronal degeneration. *J. Neurosci.* 18: 5804–5816.
57. Jensen, M. B., I. V. Hegelund, N. D. Lomholt, B. Finsen, and T. Owens. 2000. IFNγ enhances microglial reactions to hippocampal axonal degeneration. *J. Neurosci.* 20: 3612–3621.
58. Remington, L. T., A. A. Babcock, S. P. Zehntner, and T. Owens. 2007. Microglial recruitment, activation, and proliferation in response to primary demyelination. *Am. J. Pathol.* 170: 1713–1724.